Oncogene (2002) 21, 7824–7830

www.nature.com/onc

Modulation of invasive properties of human glioblastoma cells stably expressing amino-terminal fragment of urokinase-type plasminogen activator

Sanjeeva Mohanam[1], Nirmala Chandrasekar[1], Niranjan Yanamandra[1], Siddique Khawar[2], Faiz Mirza[1], Dzung H Dinh[2], William C Olivero[2] and Jasti S Rao*[,1,2]

[1]*Division of Cancer Biology, Department of Biomedical and Therapeutic Sciences, University of Illinois College of Medicine at Peoria, Peoria, Illinois, USA;* [2]*Department of Neurosurgery, University of Illinois College of Medicine at Peoria, Peoria, Illinois, USA*

The binding of urokinase-type plasminogen activator (uPA) to its receptor (uPAR) on the surface of tumor cells is involved in the activation of proteolytic cascades responsible for the invasiveness of those cells. The diffuse, extensive infiltration of glioblastomas into the surrounding normal brain tissue is believed to rely on modifications of the proteolysis of extracellular matrix components; blocking the interaction between uPA and uPAR might be a suitable approach for inhibiting glioma tumorigenesis. We assessed how expression of an amino-terminal fragment (ATF) of uPA that contains binding site to uPAR affects the invasiveness of SNB19 human glioblastoma cells. SNB19 cells were transfected with an expression plasmid (pcDNA3-ATF) containing a cDNA sequence of ATF-uPA. The resulting ATF-uPA-expressing clones showed markedly less cell adhesion, spreading, and clonogenicity than did control cells. Endogenous ATF expression also significantly decreased the invasive capacity of transfected glioblastoma cells in Matrigel and spheroid-rat brain cell aggregate models. ATF-uPA transfectants were also markedly less invasive than parental SNB19 cells after injection into the brains of nude mice, suggesting that competitive inhibition of the uPA-uPAR interaction on SNB19 cells by means of transfection with ATF cDNA could be a useful therapeutic strategy for inhibiting tumor progression.
Oncogene (2002) **21,** 7824–7830. doi:10.1038/sj.onc.1205893

Keywords: ATF; uPA; glioblastoma; invasiveness

Introduction

uPA is secreted as an enzymatically inactive single-chain proenzyme and binds to its natural ligand, the uPA receptor (uPAR). The binding of uPA to uPAR not only increases the enzymatic activity of uPA but also triggers a focal and directional proteolysis of extracellular matrix. uPA binds to uPAR by its amino-terminal fragment (ATF) in an interaction that involves the EGF-like domain (residues 1–46) and exhibits species specificity between mice and humans (Quax *et al*., 1998). Several strategies including the use of active site inhibitors, antibodies to uPA, and oligonucleotides or RNA directed against uPA have been used to affect the proteolytic activity or reduce the expression of uPA in tumor cells (Schmitt *et al*., 2000). Other attempts to abrogate the uPA/uPAR interaction use synthetic uPA-derived peptides encompassing the binding region of uPA to uPAR (Burgle *et al*., 1997) or recombinant soluble uPAR as a scavenger for uPA (Kruger *et al*., 2000).

Tumor biology studies demonstrate a tumor suppressive role for ATF at the levels of tumor invasion and metastasis. Periodic intraperitoneal injection of an ATF-immunoglobulin G conjugate has been shown to inhibit lung metastasis of human PC3 prostate carcinoma cells, with no significant effect on primary tumor growth, in athymic mice (Crowley *et al*., 1993). In another study, multiple intraperitoneal injections of a peptide from murine ATF after subcutaneous inoculation with Lewis lung carcinoma cells significantly inhibited metastatic lung tumor colonization in a dose-dependent manner (Kobayashi *et al*., 1994). In a recent study, the invasiveness of a highly metastatic human lung giant-cell carcinoma cell line transfected with ATF cDNA was significantly inhibited *in vitro*, as was the lung metastasis of implanted cells in a spontaneous metastasis model (Zhu *et al*., 2001). Li *et al*. (1998) also showed that adenovirus-mediated delivery of ATF suppressed growth of xenografted MDA-MB-231 human breast cancer cells or xenografted c57/BL6 syngeneic Lewis lung carcinoma cells grown in athymic mice.

Bifunctional inhibitors that include ATF or uPA-derived peptides covering the human uPAR binding sequences are efficient inhibitors of the uPA–uPAR interaction. ATF conjugated with a plasmin inhibitor strongly inhibited plasmin activity at the surface of smooth muscle cells and reduced the migration of those cells (Quax *et al*., 2001). ATF can also act as a growth

*Correspondence: JS Rao, Division of Cancer Biology, Department of Biomedical and Therapeutic Sciences, University of Illinois College of Medicine at Peoria, One Illini Drive, Peoria, Illinois, IL 61656-1649, USA; E-mail: jsrao@uic.edu
Received 8 May 2002; revised 12 July 2002; accepted 18 July 2002

factor for osteoblasts (Rabbani *et al*., 1992). In contrast, ATF did not impart growth factor-like signals to 8701-BC breast carcinoma cells but rather restricted the invasion of these cells *in vitro* (Luparello and del Rosso, 1996). At present, the effect of ATF on glioblastoma cell invasiveness is poorly understood.

We showed previously that uPA is overexpressed in glioblastoma cell lines and tumor tissues (Mohanam *et al*., 1993; Yamamoto *et al*., 1994a). Selective inhibition of the uPA–uPAR interaction may be an effective means of decreasing the invasiveness of human glioblastoma cells. The underlying molecular mechanism of ATF remains elusive, and the role of ATF in glioma cells has not been studied. To address this gap, we generated stable, ATF-expressing transfectants of the glioblastoma cell line SNB19 and tested whether the interaction of uPA and uPAR could be blocked by ATF, and hence whether the invasiveness of tumor cells *in vitro* would be suppressed after ATF expression. We also sought to establish whether expression of the ATF fragment would reduce the tumorigenicity of the transfected cells in a nude mouse model.

Results

Transfection of SNB19 cells with ATF-uPA cDNA increases the expression of ATF mRNA and protein

We stably transfected the human glioblastoma cell line SNB19 with the pcDNA3 vector containing cDNA of ATF-uPA and grew the cells in medium containing G418 to allow selection of drug-resistant colonies. Parental cells and clones transfected with an empty vector served as controls.

To verify that the ATF-uPA-transfected clones express ATF mRNA, we used semiquantitative reverse transcriptase–polymerase chain reaction to characterize ATF mRNA expression. Cells that had been transfected with the ATF-uPA vector showed mRNA transcripts for ATF, whereas parental cells and the vector-only transfectants did not (Figure 1). GAPDH, used as a control, was detected in all cell lines. To confirm that transfection with the ATF construct also resulted in expression of uPA protein, we used Western blot analysis of conditioned media and found that the ATF protein band was observed only in the medium from ATF-uPA stable transfectants (ATF-3, ATF-6, and ATF-11 in Figure 2a) and not in media from the empty vectors-transfected or parental cell lines. The ATF antibody recognized ATF-uPA transcript but uPA was below detectable level. Finally, to confirm that ATF produced by the transfectants was interacting directly with uPAR on the cell surface, the cells were washed extensively, eluted with acid buffer, and probed for ATF by Western blotting. Again, ATF was found in the ATF-transfected clones but not in the control cell lines (Figure 2b), indicating that the ATF secreted by the transfected cells was able to bind on the surface of those cells.

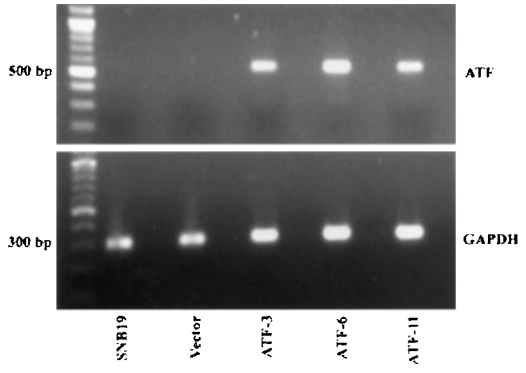

Figure 1 Detection of ATF-uPA mRNA after transfection. RT–PCR analysis of ATF-uPA transcripts in parental SNB19 cells, cells transfected with empty vector, and cells transfected with ATF-uPA cDNA. Top panel, ethidium bromide staining of RT–PCR product of the ATF-uPA RNA. Lower panel, RT–PCR product of the GAPDH RNA

Secretion of ATF reduces cell surface-associated uPA activity

ATF competes with uPA for binding to uPAR. To determine whether endogenously expressed ATF binds to uPAR and displaces uPA, we studied cell surface-associated uPA by washing the cells thoroughly with serum-free medium, extracting them with acid buffer (pH 3.0), and analysing cell surface-associated uPA activity by fibrin zymography. Cell-surface uPA activity was much lower in the ATF-transfected SNB19 cells than in the parental or vector-control cells (Figure 3).

ATF expression alters adhesion, spreading, and colony formation

After we discovered that the ATF transfectants had reduced cell surface-associated uPA activity, we tested them for adhesion and spreading capabilities. Consid-

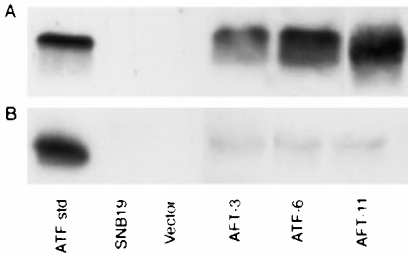

Figure 2 (**a**) Detection of ATF-uPA protein after transfection, assessed by Western blotting. Serum-free medium was collected, samples were separated under nonreducing conditions by 15% SDS–PAGE and transferred to nitrocellulose membranes. The membranes were probed with anti-ATF monoclonal antibodies and secondary antibodies (anti-mouse horseradish peroxidase) as required and developed according to enhanced chemiluminescence protocol. Purified amino-terminal fragment of uPA protein (ATF std) was used as standard marker. (**b**) Detection of ATF-uPA on the surface of stable transfectants. Parental cells, vector-transfected controls, and ATF transfectants were washed thoroughly, eluted with glycine-HCl buffer, pH 3.0, neutralized with 0.5 M HEPES buffer and analysed for the presence of ATF by Western blotting

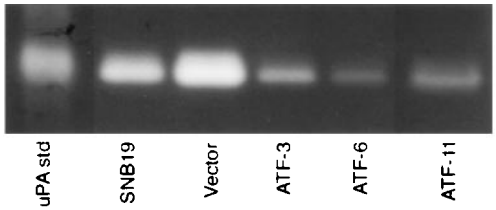

Figure 3 ATF expression reduces cell surface-associated uPA activity in SNB19 cells. Fibrin zymography of acid buffer eluates from parental SNB19 cells and various transfected clones. The cells were washed and the cell surface-associated proteins eluted with acid buffer (pH 3.0) and neutralized with 0.5 M HEPES buffer. The acid-buffer eluates were run on 10% SDS–PAGE containing plasminogen and fibrinogen to assess variations in cell surface-associated uPA activity

ered in comparison with the maximally adhering empty vector-transfected SNB19 cells (100%), the transfectant clone ATF-3 were much less adherent (33%) and the ATF-11 and ATF-6 clones were somewhat less adherent (53 and 62%, respectively) (Figure 4). Expression of ATF through transfection also reduced cell spreading (Figure 5) and colony formation after 2 weeks in culture (Figure 6).

Changes in actin cytoskeleton organization due to ATF expression

Because the cytoskeleton plays a major role in cell spreading, we next examined stress-fiber reorganization in parental cells and G418-resistant ATF-transfected clones to determine whether the change in cell adhesion resulted from changes in cytoskeleton organization. In the ATF stable transfectants, stress-fiber organization was severely disrupted, as evidenced by the absence of networks of stress fibers forming during cell spreading (Figure 7).

Decreased invasive potential among transfected clones

Since ATF interferes with the interaction between uPA with uPAR, we assessed its ability to inhibit cell invasion *in vitro* in Matrigel and spheroid coculture invasion assays. No marked differences in invasiveness were noted between the parental cells and the vector-transfected control cells in either assay. However, the invasive potential of the ATF-uPA-transfected clones was substantially inhibited in both assays. In the Matrigel assay, quantitative analysis of invading cells by 3-(4,5-dimethylthiazol-2-yl)-2,5-diphenyltertrazolium bromide (MTT) indicated that at 48 h, 45% of the parental cells and 42% of the empty-vector-transfected clones had traversed the membrane; in contrast, the invasiveness of the ATF-transfected clones was greatly reduced (10% ATF-3, 25% ATF-6, and 16% AFT-11) (Figure 8). In the spheroid coculture assays, spheroids consisting of parental SNB19 cells or vector transfectants attached to and invaded the fetal rat brain aggregates by 72 h of coculture, but spheroids consisting of the ATF-expressing clones did not (Figure 9a).

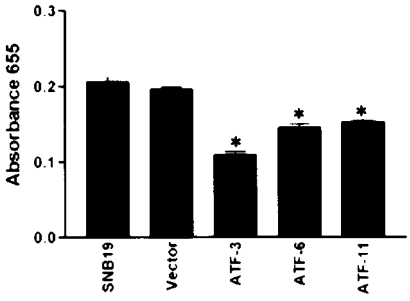

Figure 4 ATF expression reduces cell adhesion. Parental and transfectants were allowed to adhere tissue culture plates for 2 h at 37°C and the proportions of adhering cells were determined. The experiments were done twice. Data points represent the means of quadruplicate determinations (±s.d.) and are expressed as a percentage of control. $*P<0.01$

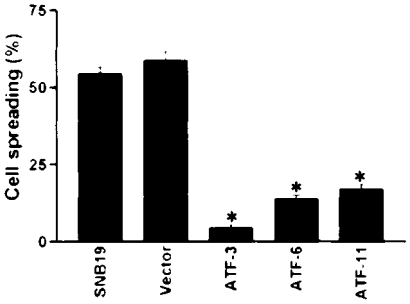

Figure 5 ATF expression limits cell spreading. Cells were added to 96-well microtiter plates and allowed to attach and spread for 2 h, after which the cells were fixed and analysed by phase contrast microscopy. The experiments were repeated twice and values represent the means of quadruplicate determinations (±s.d.) $*P<0.01$

Expression of ATF reduces tumor growth in nude mice

Finally, to determine whether the expression of ATF is associated with inhibition of tumor growth *in vivo*, we injected the brains of nude mice with parental SNB19 cells, vector-transfected controls, or ATF-transfected cells and assessed the growth of the implanted cells. All mice injected with parental SNB19 cells developed tumors. In contrast, mice injected with the ATF-3 transfectant showed markedly reduced tumor formation at 4 weeks after injection; the presence of smaller tumors was confirmed by histologic examination (Figure 9b).

Discussion

The coordinated interaction of different proteolytic systems is important for tumor cell invasion and metastasis (Duffy, 1996). The invasive capacity of tumor cells can be suppressed by synthetic inhibitors directed against various proteases or by plasminogen activator system antagonists (Min *et al*., 1996; Festuccia *et al*., 1998). The uPA system has pivotal roles in tumor growth, angiogenesis, and metastasis.

Figure 6 ATF modulates colony formation by SNB19 cells. Parental SNB19 cells and stable ATF transfectants were plated (500 per 100-mm tissue culture dish) and allowed to grow for 2 weeks. The experiments were done twice. At the end of the experimental period, the colonies were stained and photographed

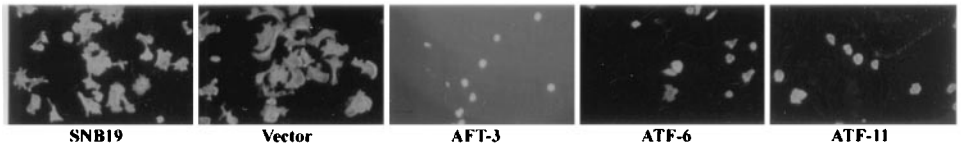

Figure 7 ATF expression disrupts stress-fiber organization in SNB19 cells. Parental cells and transfected cells were allowed to spread for 24 h, fixed with 3% paraformaldehyde, permeabilized with 0.5% Triton X-100, and stained with TRITC-phalloidin. The experiments were repeated twice

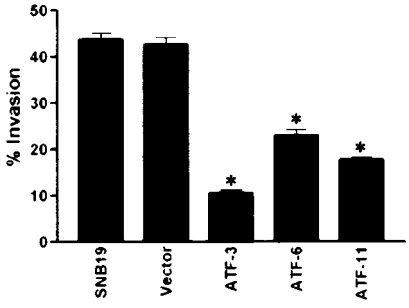

Figure 8 ATF expression inhibits the invasion of SNB19 cells through Matrigel. Cell suspensions were layered onto Matrigel-coated transwell inserts and the percentage of cells traversing the insert was calculated as a measure of invasion. Values are means $\pm$ s.d. of four determinations. $^*P<0.01$

Earlier studies focused on the proteolytic cascades initiated by uPA and mediated by the catalytic B chain, which resulted in matrix remodeling and allowed tumor cell invasion and migration (Reuning *et al*., 1998; Schmitt *et al*., 2000). The binding of uPA to uPAR has been shown to mediate various other signaling cascades (Dear and Metcalf, 1998), although the role of these cascades in tumor progression is poorly understood.

uPA and uPAR are expressed by many tumor types, and their expression correlates with tumor progression and poor prognosis (Duffy, 1996). This association is consistent with the hypothesis that plasminogen activation contributes to the invasive phenotype of tumor cells. Glioblastoma cells and tumor tissues exhibit levels of uPA and uPAR that increase in parallel with tumor grade (Yamamoto *et al*., 1994a,b). Down-regulation of uPA or uPAR in glioblastoma cells results in reductions in invasiveness and tumorigenicity (Mohanam *et al*., 1997, 2001; Go *et al*., 1997). Since the uPA–uPAR system contributes to the invasion and motility of several cell types associated with tumor progression (e.g., endothelial and tumor cells), we hypothesized that the inhibition of the uPA–uPAR interaction would have significant anti-tumor effects.

Several previous studies suggest a possible role for uPA or uPAR in cell adhesion and migration independent of the enzymatic activity of the uPA (Stahl and Mueller, 1997; Waltz *et al*., 2000). Cell adhesion and spreading are the result of cooperative actions among adhesive systems. However, until now, the direct role of blocking uPA–uPAR interaction by ATF has not been explored in glioblastoma cells. Our results demonstrate that forced expression of ATF in glioma cells led to decreased cell adhesion, which could be due to the reduction in number of uPA–uPAR complexes. The molecular mechanism by which ATF affects cell adhesion is not yet clear, but the results presented here suggest that ATF may modulate cell adhesion and spreading by stimulating the reorganization of the cytoskeleton. Alternatively, ATF expression could have a regulatory function in adhesion-induced signal transduction events, which in turn lead to a reorganization of the cytoskeleton. We monitored endogenous ATF-induced reorganization of the actin cytoskeleton by rhodamine-labeled phalloidin staining and found that expression of ATF also had a significant effect on actin reorganization in SNB19 glioblastoma cells. The parental cells showed intensely staining, closely packed fine microfilament bundles oriented to the long axes of the cells and terminating at focal contacts. The ATF-transfected cells, in contrast, exhibited membrane ruffling and irregular networks of microfilaments throughout the cytoplasm but did not form focal adhesions or actin stress fibers. Notably, intensification of adhesion-induced lamellae and formation of filopodia were absent in the ATF-expressing transfectants. In summary, ATF expression diminished adhesion and spreading and is associated with reorganization of the actin cytoskeleton.

Tumor cell invasiveness is a complex multistep process that involves cell adhesion, proteolysis of the

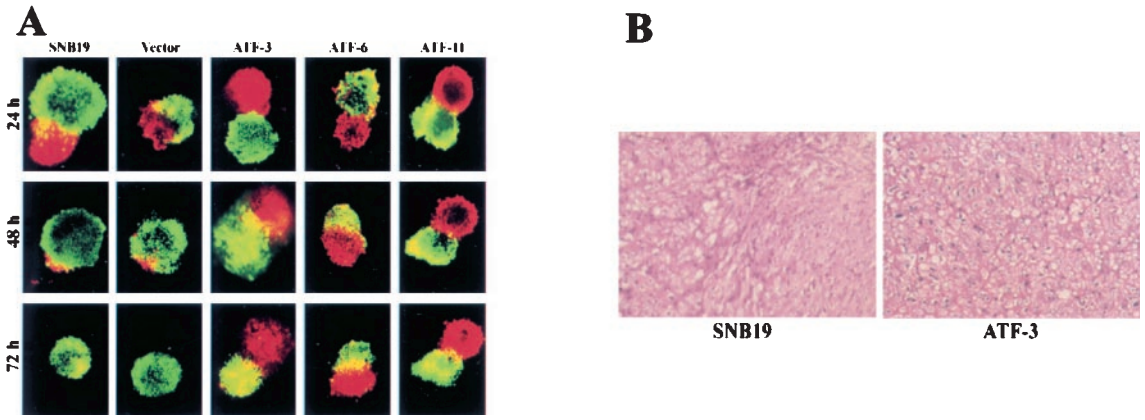

Figure 9 (**a**) ATF expression inhibits the invasion of SNB19 cells through rat-brain aggregates. Confocal laser scanning images of SNB19 spheroids and rat-brain aggregate cocultures scanned at a depth of 100 μm from the spheroid surface. The rat-brain aggregates appear green and the tumor cell spheroids appear red. Four–five tumor spheroid/rat brain aggregate confrontations were carried out in each group to confirm the reproducibility. (**b**) Tumorigenicity of parental and ATF-transfected SNB19 (ATF-3) cells in the brains of nude mice. Five mice were injected in each group and after 4 weeks the mice were sacrificed, tumors tissues were removed, sectioned and stained. A photomicrograph of a tumor section stained with hematoxylin and eosin shows that tumors that formed in tissues derived from ATF-transfected cells injected into the mouse brain were much smaller than those derived from the parental SNB19 cells. All the animals examined in each group showed identical results

extracellular membrane and basement membrane, and migration of cells through the disrupted matrix. Several studies have demonstrated the pivotal role of the uPA/uPAR system in the invasiveness of tumor cells *in vitro* and *in vivo* (Andreasen *et al*., 1997). In this study, we showed that expression of ATF by cDNA transfection reduced cellular invasiveness in both Matrigel and spheroid coculture invasion assays. These findings are in accord with earlier reports of ATF expression in a human lung giant-cell carcinoma cell line (Zhu *et al*., 2001). Our results with the Matrigel assay support the idea that the interaction of uPA with the cell surface is crucial for invasion through Matrigel, which contains a mixture of extracellular membrane components. To confirm these findings, we used a three-dimensional spheroid coculture model that more closely mimics *in vivo* invasion into a complex and intact extracellular membrane synthesized by fetal rat brain aggregates. We confirmed that spheroids from the ATF-transfectants invaded fetal rat brain aggregates to a much lesser extent than did spheroids from parental and vector control cells. The efficacy of ATF in suppressing invasiveness may lie in the possibility that ATF has additional effects apart from its direct effect on blocking uPA to its receptor, such as decreasing plasminogen activation by making uPAR less accessible for uPA or inhibiting the plasmin-mediated activation of other matrix-degrading enzymes such as proenzyme forms of matrix metalloproteinases. Since localized plasmin inhibition seems to be an essential route to inhibiting invasion, ATF is an interesting candidate for therapeutic inhibition of cell invasiveness.

If the presence of cell surface-bound uPA is a key determinant of invasion, then inhibiting the interaction of uPA with uPAR should translate into a measurable reduction in invasiveness. Thus, blocking the binding of uPA to uPAR by the expression of ATF could reduce the proteolysis mediated by cell surface-associated uPA in tumor cells. We tested the tumorigenicity of parental cells and ATF transfectants in nude mice with an intracerebral implantation method; the ATF transfectants formed smaller tumors than did parental cells, which showed typical invasive behavior and progressive tumor growth. Earlier, lung dissemination of Lewis lung carcinoma cells was shown to be significantly reduced after intratumoral injection of an adenovirus containing murine ATF at the primary site; also, systemic administration of this construct inhibited subsequent liver metastasis in a LS174T human colon carcinoma xenograft model (Li *et al*., 1998). We also found that endogenous expression of ATF reduced cell adhesion, cell spreading, and colony formation as well as suppressing tumor growth. In our study, ATF is found associated with cells suggesting that it may interact with uPAR. Because the uPAR and uPA molecules associated with the plasminogen activation system on the cell surface are of fundamental importance in cell biology, the addition of an antagonist of plasminogen activators such as ATF may not only shift the balance in the enzymatic activity of the uPA–uPAR complex, but may also trigger further cellular responses. Our study indicates that the inhibition of uPA–uPAR interaction, a key step in tumor progression, could constitute a new therapeutic approach for the control of both tumor cell growth and invasion.

Materials and methods

Cell cultures

SNB19 glioblastoma cells were maintained in Dulbecco's modified Eagle's medium supplemented with 10% fetal calf serum in a humidified atmosphere containing 5% CO_2 at 37°C and subcultured every 3–5 days.

Preparation of constructs

A cDNA fragment encoding amino acids 1–155 of uPA, isolated by polymerase chain reaction (PCR) with sense (5′-ATAAGCTTGCCGCCGTCTAGCGCCCCGA-3′ including an *Hind*III site) and antisense (5′-GCGGATCCTCA-CTTTTTTCCATCTGCGCAGTC 3′ including *BamH*I site) primers was subcloned into *Hind*III and *BamH*I cut pcDNA3 expression vector (Invitrogen, Carlsbad, CA, USA). The orientation and sequence of the insert was confirmed by automated sequencing.

Transfection of SNB19 cells

The SNB19 cells were transfected with the ATF-uPA pcDNA3 construct or with pcDNA3 vector alone by using lipofectin (Invitrogen, Carlsbad, CA, USA) as described elsewhere (Mohanam *et al*., 1997). Stable transfectants were initially selected by using cloning cylinders after 3–4 weeks of culture in medium containing G418 (800 μg/ml).

Reverse transcriptase–polymerase chain reaction

Cells were washed with ice-cold PBS and total RNA was extracted with the TRIzol reagent (Invitrogen, Carlsbad, CA, USA). RNA was first treated with DNase at 37°C for 1 h and then reverse-transcribed by using a cDNA cycle kit (Invitrogen, Carlsbad, CA, USA) and random primers. To amplify the cDNA, a 1-μl aliquot of the reverse-transcribed cDNA was subjected to 30 cycles of RT–PCR in 25 μl of PCR Master Mix (Promega, Madison, WI, USA) buffer containing 100 ng of sense and antisense primers. The efficiency of cDNA synthesis was estimated by RT–PCR with GAPDH-specific primers. The following sense (S) and antisense (AS) primers were used in RT–PCR reactions: ATF (S, 5′-ATAAGCTTGCCGCCGTCTAGCGCCCCGA; AS, 5′-GCGGATCCTCACTTTTTTCCATCTGCGCAGTC-3′; amplicon size 524 bp); GAPDH (S, 5′-CGGAGTCAACG-GATTTGGTCGTAT-3′; AS, 5′-AGCCTTCTCCATGGT-GGTGAAGAC-3′; amplicon size 307 bp). Samples were subjected to electrophoresis on a 1.5% agarose gel and photographed as ethidium bromide fluorescent bands.

Electrophoresis and Western blot analysis

Equal amounts of protein from serum-free media were loaded onto 15% minigels and separated by sodium dodecyl sulfate polyacrylamide gel electrophoresis (SDS–PAGE). Resolved proteins were electrophoretically transferred to nitrocellulose membrane (BioRad, Hercules, CA, USA). The membrane was then blocked with 5% lowfat dry milk in TBS-T (10 mM Tris pH 7.2, 50 nM NaCl, 0.2% Tween 20) for 1 h at room temperature and incubated with primary antibody at 4°C for 18 h. Blots were washed extensively with TBS-T and incubated with 1 : 5000 dilution of horseradish peroxidase (HRP)-conjugated secondary antibody (Amersham Pharmacia Biotech, Piscataway, NJ, USA) diluted in TBS-T containing 3% BSA for 1 h at room temperature. Labeled proteins were visualized by enhanced chemiluminescence (Amersham Pharmacia Biotech, Piscataway, NJ, USA). Mouse monoclonal antibodies against human ATF were obtained from American Diagnostica (Greenwich, CT, USA).

Fibrin zymography

The enzymatic activity and molecular weight of electrophoretically separated forms of PA were determined in acid-wash extracts and conditioned medium of all the clones and parental cells by SDS–PAGE as described previously (Mohanam *et al*., 1997). Briefly, the SDS–PAGE gel contains acrylamide to which purified plasminogen and fibrinogen were added as substrates before polymerization. After polymerization, equal amounts of proteins in the samples were electrophoresed and the gel was washed twice with 2.5% Triton X-100 for 30 min each time, and the gel was incubated at 37°C overnight with glycine buffer (pH 7.5). After staining with Coomassie blue and destaining, the final gel has a uniformly blue background except in regions to which PAs have migrated and activated the plasminogen to form plasmin.

Cell spreading

Cells suspended in serum-free medium were added to 96-well microtiter plates (10^4 cells per well) and allowed to attach and spread for 2 h. After this incubation, the medium containing non-adhered cells was poured off and the cells were fixed for 30 min with a solution of 3.7% formaldehyde and 5% sucrose. The cells in at least three parallel fields in each of four wells were analysed by phase contrast microscopy. An individual cell was counted as having spread when its diameter was at least twice that of the nucleus. The percentage of spread cells was evaluated as (number of spread cells divided by total of number cells in field $\times 100 =$ percentage of spreading.

Adhesion assays

Cells were harvested, washed three times with serum-free medium, and allowed to adhere tissue culture plates for 2 h at 37°C. Cells were then washed three times with HEPES buffer and fixed with 2.5% formaldehyde in PBS, stained with 0.5% crystal violet in 20% (v/v) methanol/water, and viewed under a microscope. The amount of bound cells was estimated by solubilizing the dye with 0.1 M sodium citrate and reading the absorbance at 570 nm. Quadruplicate determinations were done for each condition and analysed for statistical significance

Staining of actin cytoskeleton

Cells were fixed in 3% paraformaldehyde in phosphate-buffered saline for 15 min followed by permeabilization with 0.5% Triton X-100 in phosphate-buffered saline for 5 min. After being washed three times with phosphate-buffered saline, the specimens were incubated with rhodamine-conjugated phalloidin for 30 min. Staining of actin was observed under a confocal laser scanning microscope (Olympus, Tokyo, Japan).

Colony formation

Cells (4×10^3) were plated on 100-mm tissue culture dishes and the medium was changed every 3 days. After 2 weeks, the resulting colonies were fixed in methanol and stained with Hema-3.

Matrigel invasion assay

Cells were plated on Matrigel-coated cell-culture inserts in Transwell chambers (Corning Inc, Corning, NY, USA) containing 12-mm filters (pore size 8 μm) as follows. Matrigel (Beckton Dickinson, Bedford, MA, USA) was diluted with cold, serum-free medium and 150 μg was applied to each

filter, which were then dried in a hood and incubated at 37°C for 30 min. Cells (1×10^5) were suspended in serum-free medium, added to the Matrigel-coated chamber, and conditioned medium was placed in the lower chamber as a chemoattractant. After incubation for 48 h at 37°C in 5% CO_2, the Matrigel-coated side of the filter was removed with a cotton swab and cells on the opposite side of the filter were fixed in 10% formaldehyde, stained with hematoxylin and eosin, and counted. Each assay was performed in quadruplicate.

Coculture invasion assay

Spheroids of fetal rat brain cells and tumor cells were prepared as described elsewhere (Go *et al*., 1997). Briefly, brain cells obtained from 18-day-old fetuses of Sprague-Dawley rats were cultured for 16 days, after which aggregates 100–200 μm in diameter were selected for the experiments. Fetal brain cell aggregates were stained with 3,3′-dioctadecyloxacarbocyanine perchlorate (DiO). Multicellular tumor-cell spheroids of parental cells, empty-vector-transfectants, and uPA-ATF stable transfectants were grown separately on 0.75% agar-coated plates and stained with 1,1 dioctadecyl-3.3.3′.3′-tetramethylindocarbocyanine perchlorate (DiI). For the coculture, the DiI-stained tumor spheroids and DiO-stained fetal rat-brain aggregates were washed in medium and transferred in quadruplicate to individual wells of a 96-well plate that had been base-coated with agar. A sterile syringe and stereomicroscope were used to place the tumor spheroids and fetal rat-brain aggregates in close contact with each other. At different times thereafter, serial optical sections were obtained from the surface to the center of the cocultures by confocal laser-scanning microscopy, and the extent of invasion was monitored.

In vivo *inhibition of tumor growth*

A midline scalp incision was made in nude mice, and a burr hole was made with an electric drill 2.5 mm lateral to the sagittal suture and at the coronal suture. A 10-μl cell suspension containing 2×10^6 cells in serum-free medium was injected with a Hamilton syringe attached to a stereotactic frame at a depth of 3 mm. After the cells were injected, the burr hole was sealed with sterile bone wax and the scalp closed. The mice were anesthetized and killed at 4 weeks after injection. The brains were removed, fixed in 4% formaldehyde, and sliced into sections and embedded in microscopic slides. The sections were stained with hematoxylin and eosin to reveal the tumor growth.

Acknowledgments
We thank Karen Minter for preparing the manuscript. This work was supported by National Cancer Institute grants CA76350, CA75557 and CA85216 (to JS Rao).

References

Andreasen PA, Kjoller L, Christensen L and Duffy MJ. (1997). *Int. J. Cancer,* **72,** 1–22.
Burgle M, Koppitz M, Riemer C, Kessler H, Konig B, Weidle UH, Kellermann J, Lottspeich F, Graeff H, Schmitt M, Goretzki L, Reuning U, Wilhelm O and Magdolen V. (1997). *J. Biol. Chem.,* **378,** 231–237.
Crowley CW, Cohen RL, Lucas BK, Liu G, Shuman MA and Levinson AD. (1993). *Proc. Natl. Acad. Sci. USA.,* **90,** 5021–5025.
Dear AE and Medcalf RL. (1998). *Eur. J. Biochem.,* **252,** 185–193.
Duffy MJ. (1996). *Clin. Cancer Res.,* **2,** 613–618.
Festuccia C, Dolo V, Guerra F, Violini S, Muzi P, Pavan A and Bologna M. (1998). *Clin. Exp. Metastasis,* **16,** 513–528.
Go Y, Chintala SK, Mohanam S, Gokaslan Z, Venkaiah B, Bjerkvig R, Oka K, Nicolson GL, Sawaya R and Rao JS. (1997). *Clin. Exp. Metastasis,* **15,** 440–446.
Kobayashi H, Gotoh J, Fujie M, Shinohara H, Moniwa N and Terao T. (1994). *Int. J. Cancer,* **57,** 727–733.
Kruger A, Soeltl R, Lutz V, Wilhelm OG, Magdolen V, Rojo EE, Hantzopoulos PA, Graeff H, Gansbacher B and Schmitt M. (2000). *Cancer Gene Ther.,* **7,** 292–299.
Li H, Lu H, Griscelli F, Opolon P, Sun LQ, Ragot T, Legrand Y, Belin D, Soria J, Soria C, Perricaudet M and Yeh P. (1998). *Gene. Ther.,* **5,** 1105–1113.
Luparello C and Del Rosso M. (1996). *Eur. J. Cancer,* **32A,** 702–707.
Min HY, Doyle LV, Vitt CR, Zandonella CL, Stratton-Thomas JR, Shuman MA and Rosenberg S. (1996). *Cancer Res.,* **56,** 2428–2433.
Mohanam S, Chintala SK, Go Y, Bhattacharya A, Venkaiah B, Boyd D, Gokaslan ZL, Sawaya R and Rao JS. (1997). *Oncogene,* **14,** 1351–1359.
Mohanam S, Jasti SL, Kondraganti SR, Chandrasekar N, Kin Y, Fuller GN, Lakka SS, Kyritsis AP, Dinh DH, Olivero WC, Gujrati M, Yung WK and Rao JS. (2001). *Clin. Cancer Res.,* **7,** 2519–2526.
Mohanam S, Sawaya R, McCutcheon I, Ali-Osman F, Boyd D and Rao JS. (1993). *Cancer Res.,* **53,** 4143–4147.
Quax PH, Grimbergen JM, Lansink M, Bakker AH, Blatter MC, Belin D, van Hinsbergh VW and Verheijen JH. (1998). *Arterioscler. Thromb. Vasc. Biol.,* **18,** 693–701.
Quax PH, Lamfers ML, Lardenoye JH, Grimbergen JM, de Vries MR, Slomp J, de Ruiter MC, Kockx MM, Verheijen JH and van Hinsbergh VW. (2001). *Circulation,* **103,** 562–569.
Rabbani SA, Mazar AP, Bernier SM, Haq M, Bolivar I, Henkin J and Goltzman D. (1992). *J. Biol. Chem.,* **267,** 14151–14156.
Reuning U, Magdolen V, Wilhelm O, Fischer K, Lutz V, Graeff H and Schmitt M. (1998). *Int. J. Oncol.,* **13,** 893–906.
Schmitt M, Wilhelm OG, Reuning U, Kruger A, Harbeck N, Lengyel E, Graeff H, Gansbacher B, Kessler H, Burgle M, Sturzebecher J, Sperl S and Magdolen V. (2000). *Fibrinol. Proteol.,* **14,** 114–132.
Stahl A and Mueller BM. (1997). *Int. J. Cancer,* **71,** 116–122.
Waltz DA, Fujita RM, Yang X, Natkin L, Zhuo S, Gerard CJ, Rosenberg S and Chapman HA. (2000). *Am. J. Respir. Cell Mol. Biol.,* **22,** 316–322.
Yamamoto M, Sawaya R, Mohanam S, Bindal AK, Bruner JM, Oka K, Rao VH, Tomonaga M, Nicolson GL and Rao JS. (1994a). *Cancer Res.,* **54,** 3656–3661.
Yamamoto M, Sawaya R, Mohanam S, Rao VH, Bruner JM, Nicolson GL and Rao JS. (1994b). *Cancer Res.,* **54,** 5016–5020.
Zhu F, Jia S, Xing G, Gao L, Zhang L and He F. (2001). *DNA Cell Biol.,* **20,** 297–305.